

Growth and Characterization of Cerium Doped Zinc Oxide Nanocrystalline Thin Film.

ALI FATIMA. A* and SUGANTHI DEVADASON

Department of Physics, Karunya University, Coimbatore - 641 114, Tamilnadu, India.
E.mails : ali_41070@rediff.com* and suganthi@karunya.edu

ABSTRACT

Zinc oxide and cerium doped zinc oxide (ZnO:Ce) thin films were deposited on glass substrates using the sol-gel spin coating technique. Films were deposited at 200°C using zinc acetate as the precursor solution. The effect of doping concentration of Cerium on the structural and optical properties of ZnO films has been reported. X-ray diffraction studies show a change in preferential orientation from the (002) to the (100) and (101) crystal planes with increase in cerium doping concentration. The grain size and lattice constants have been derived from XRD studies. Optical characteristics of the films have been studied using spectrophotometer in the wavelength range 300-800nm. These films exhibited good transparency in the visible and infrared region. The average transmittance increased as the doping concentration increased. Photoluminescence spectra of bare and doped zinc oxide films were studied.

Key words: Zinc oxide, sol-gel, X-ray diffraction, lattice constant, Photoluminescence.

1. INTRODUCTION

ZnO is a direct band-gap semiconductor with a wurtzite structure. Zinc oxide based coatings are of much interest in science and technology due to their interesting potential applications in spintronic devices such as non-volatile memories, spin valve transistors, and ultrafast optical switches¹⁻³, solar cells, gas sensors⁴⁻⁶, etc. The remarkable properties of ZnO are its wide direct-band gap of 3.37 eV and the exciton binding energy of 60 meV,

which makes it an excellent material for excitonic devices. The most commonly occurring lanthanide (rare earth) is cerium, which is used as a dopant because rare earth compounds have been widely used as high-performance luminescent devices, magnets, catalysts, and other functional materials^{8,9}. Many techniques have been employed to produce the ZnO thin film including chemical vapour deposition⁷ molecular beam epitaxy⁸, metal organic chemical vapor deposition⁹, radio frequency magnetron sputtering¹⁰, spray pyrolysis^{11,12}

and sol-gel¹³ methods. The sol gel method is effective for thin film ZnO growth because high vacuum is not required, and equipments costs are low.

In the present work, undoped and Ce-doped ZnO poly crystalline films were successfully grown by sol gel spin coating at temperature of ~ 200 °C. The samples were examined by X-ray diffraction (XRD), UV-Vis and photoluminescence (PL) measurements for structural and optical characterization.

2. EXPERIMENTAL PROCEDURES

Sol-gel spin coating technique was used to obtain doped zinc oxide thin films. Precursor solution of 0.5M zinc acetate was mixed with ethanol and diethanolamine (DEA).. The compound source of dopant,

cerium (III) nitrate was added to the above solution by varying the dopant concentration of Ce between 1 to 3%. The solution was stirred well with a magnetic stirrer for 1 h at 50°C and was further cooled to room temperature. The solution was finally aged at room temperature for 24 h. Ce-doped ZnO films were prepared on glass substrate by repeated coating and the procedure followed is explained. Spin coating was performed at room temperature, with a rate of 3000 rpm for 30 s. After each deposition, the films were heated in an open atmosphere at 200°C for 1 min to remove the moisture content in the film. The above said coating process was repeated for eight times and the films were finally post heated at 450°C for 1h in open air atmosphere using a heater coil of 2000W.

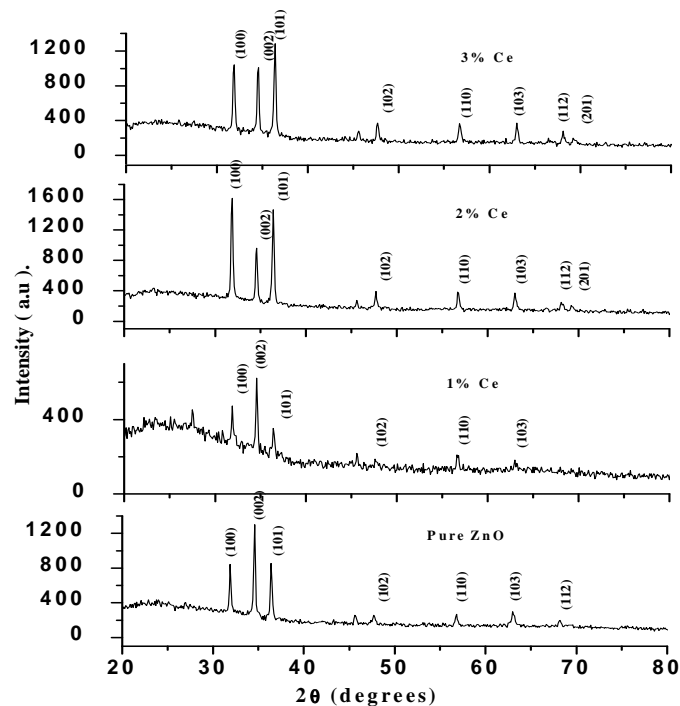


Figure 1: XRD patterns of ZnO and Ce doped ZnO

XRD measurements were performed to identify the structure and crystalline behaviour of the films. The optical measurements of the Ce-doped ZnO thin films were carried out at room temperature using Jasco UV-VIS-NIR spectrophotometer in the wavelength range of 300 to 800nm. Room temperature Photoluminescence (PL) studies was carried out using the Varian Cary Eclipse Fluorescence spectrophotometer.

3. RESULTS AND DISCUSSION

3.1. Structural properties

In the XRD patterns of the undoped and Ce-doped ZnO thin films shown in

Figure 1, the peaks are identified as (1 0 0), (0 0 2),(1 0 1), (1 0 2), (1 1 0), (1 0 3) ,(1 1 2) and (2 0 1) reflection planes corresponding to wurtzite structure of ZnO, confirming that all the polycrystalline films retain the similar ZnO structure and are randomly oriented.

Xu *et al*¹⁴ have obtained only *c*-axis oriented films on glass substrate by the sol-gel technique contrary to the random orientation of the ZnO films reported in the present work. The reason for this deviation might be due to the strong influence of the precursor chemistry and heat treatment process. The value of lattice constant, *c* is calculated from the XRD data and is given in table 1. It is observed that the *c*-axis length does not change much with the increase in the doping concentration of cerium.

Table 1: Lattice constants calculated for different doping concentration

Lattice constant	Pure Zn0	1% ce doped	2% ce doped	3% ce doped
a (Å)	3.23845	3.23790	3.24273	3.24256
c (Å)	5.18538	5.18440	5.18882	5.19160

It is interesting to note that the peak position of the diffraction plane (0 0 2) is shifted towards the lower 2θ value with the increase in the Ce concentration.. The crystallite size has also been calculated using Scherrer's formula:¹⁵

$$D = \frac{0.9\lambda}{\beta \cos \theta} \quad (1)$$

where *D* is the grain size, λ is the wavelength of the x-ray radiation used, β is

the full width at half maximum (FWHM) of the diffraction peak and θ is the Bragg diffraction angle of the XRD peak. The grains are of uniform dimension and the grain sizes were found to be 29 , 28 , 29 and 31 nm, for 0.0%, 1%, 2%, and 3% of Ce doping, respectively Grain size calculated for ZnO films for various Ce-doping concentration is given in table 2.

Table 2: Grain size for different doping concentration.

Plane (hkl)	Grain size (nm)			
	Pure Zn0	1% ce doped	2% ce doped	3% ce doped
100	30	30	29	28
002	29	28	29	31
101	29	28	28	29

3.2 Optical properties

The high transmission in the visible region is a very important factor in many applications. So, the transmittance of all representative thin films was studied by UV-Vis spectroscopy at room temperature. The results show that the transmittance is higher than 70 % in all thin films in visible region. The theory of optical transmission gives the relationship between the absorption coefficient (α) and photon energy ($h\nu$) for direct transition as $(\alpha h\nu)^2 = (h\nu - E_g)^2$ where

E_g is the energy band gap. Fig. 2 shows the $(\alpha h\nu)^2$ versus $(h\nu)$ plots of pure and Ce-doped ZnO films derived from the transmission spectra. The band gap can be estimated by extrapolation of the linear portion of an $(\alpha h\nu)^2$ versus $(h\nu)$ plot. The value of the energy band gap determined from optical transmittance data is 3.13 eV for undoped ZnO thin film which is in agreement with the theoretical value. For cerium doped ZnO thin films the optical energy band gap value varies between 3.00 to 3.24 eV.

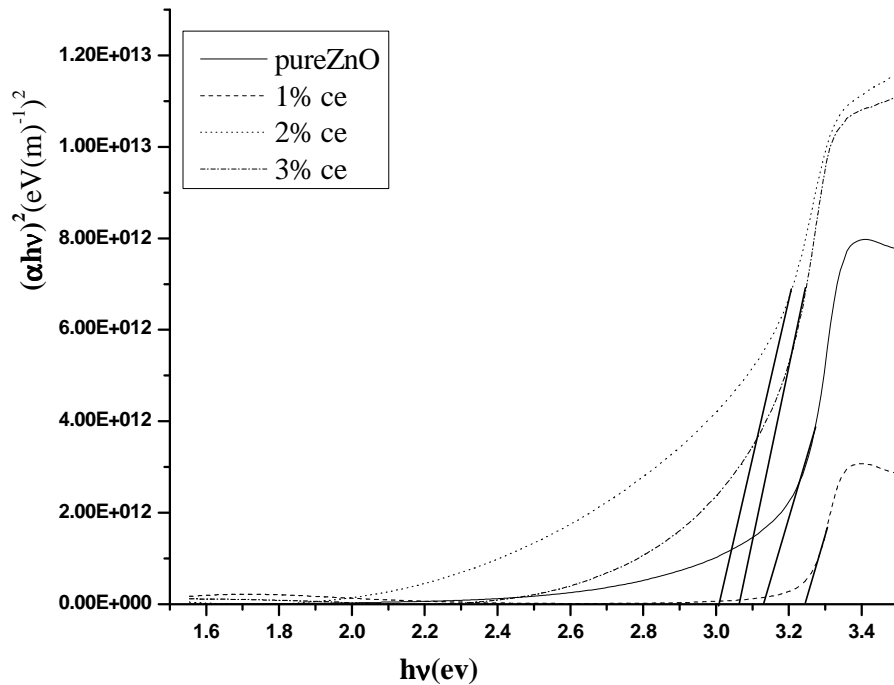


Figure 2: Plot of $(\alpha h\nu)^2$ Vs $h\nu$ for ZnO thin films

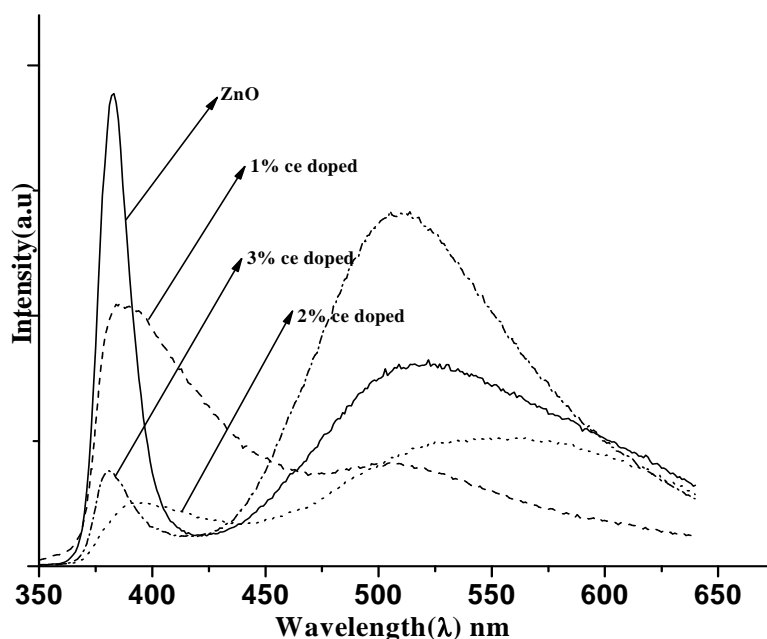


Figure 3: PL spectra of bare ZnO and Ce-doped ZnO

The technique of photoluminescence excitation has become a standard one for obtaining information on the nanostructures. The photoluminescence excitation technique involves scanning the frequency of the excitation signal, and recording the emission within a very narrow spectral range.

Figure 3 shows the photoluminescence spectra for the band-edge and deep-trap emissions. Two main features are observed. The relative strength of the band-edge photoluminescence peak compared with the deep level luminescence is clearly seen in Figure 3. The PL spectrum of the pure ZnO exhibits stronger near-band-edge (NBE) emission at 382 nm and green luminescence band centred at about 515 nm. According to the literature^{16,17}, NBE or UV-

emission typically results from the recombination of free or bound exciton indicating the high crystal quality of the material. The PL spectra of the Ce-doped exhibits a relatively weak NBE emission peaks at 384, 390 and 381 nm for 1%, 2% and 3% doping respectively compared with the pure ZnO films. The green emission band originates from the recombination of photo-generated hole with a singly ionized defect, such as oxygen vacancy^{18,19}.

4. CONCLUSION

ZnO nanocrystalline thin films have successfully been synthesized via a simple sol gel route. The grain size slightly increases from 29 to 31 nm when doped with

3% cerium . The optical transmittance was about 75% in visible range for all the films. The optical studies reveal that these films have a direct energy band gap and it is observed that the band gap energy decreases with 2% doping of cerium. The determined optical parameters are in good agreement with previously reported results. Photoluminescence spectra, showing strong and sharp near band edge emission.

REFERENCES

1. G. Glaspell, P. Dutta, and A. Manivannan, *Journal of Cluster Science*, Vol. 16, No. 4, December, 523-536 (2005).
2. J. L. Costa-Kr amer, F Briones, J. F. Fern andez, A. C. Caballero, M. Villegas, M. D iaz, M A Garc ia and A. Hernando, *Nanotechnology* 16, 214–218 (2005).
3. M. A. Garc a, F. Jim enez-Villacorta, A. Quesada, J. de la Venta, N. Carmona, I. Lorite, J. Llopis, and J. F. Fern andez, *Journal of Applied Physics* 107, 043906 (2010).
4. H. Rensmo, K.Keis, H.Lindstron, S.Sodergrem, A.Solbrand, A.Hagfeldt, S-E. Linduist, L.N.Wang, M. Muhammed, *Journal of Physics and Chemistry*, B101, 2598 (1997).
5. J.V.Asbury, Y. Wang, T. Lian, *Journal of Physics and chemistry*, B103, 6643 (1999).
6. R.L. Mishra¹, A.K. Sharma, R.K. Srivastava and S.G. Prakash *Invertis Journal of Science & Technology* Vol. 1, No. 3, 167-171 (2008).
7. Stefan Lautenschlaeger, Sebastian Eisermann, Bruno K. Meyer, Gordon Callison, Markus R. Wagner and Axel Hoffmann, *Phys. Status Solidi RRL* 3, No. 1, 16–18 (2009).
8. A. Bakin, A. Wagner, E. Schlenker, B. Postels, M. Al-Suleiman, A. Behrends, A-H Elshaer, V. Petukhov, A.Waag, 16 (12), 107 (2008).
9. N. Yoshii, A. Nakamura, S. Hosaka, J. Temmyo, *ECS Transactions*, 16 (12), 3 (2008).
10. Jae Bin Lee, Hyeong Joon Kim, Soo Gil Kim, Cheol Seong Hwang, Seong-Hyeon Hong, Young Hwa Shin, Neung Hun Lee, *Thin Solid Films* 435, 179–185 (2003).
11. Tatjana Dedova, Olga Volobujeva , Jelena Klauson ,Arvo Mere ,Malle Krunks, *Nanoscale Res Lett*, 2:391–396 (2007).
12. I. Oja Acik, A. Katerski, A. Mere, J. Aarik, A. Aidla, T. Dedova , M. Krunks, *Thin Solid Films* 517, 2443–2447 (2009).
13. Mingsong Wang, Sung Hong Hahn , Eui Jung Kim, Jae Seong Kim, Sunwook Kim, Chinho Park, Kee-Kahb Koo, *Thin Solid Films* 516, 8599–8603 (2008).
14. Z.Q. Xu, H. Deng, Y. Li, Q.H. Guo, Y.R. Li, *Materials Research Bulletin* 41, 354–358 (2006).
15. Young-Sung Kim, Weon-Pil Tai, *Applied Surface Science* 253 (2007) 4911–4916.
16. Y.C. Kong, D.P. Yu, B. Zhang, W. Fang, S.Q. Feng, *Appl. Phys.Lett.* 78, 407 (2001).
17. M.H. Huang, Y. Wu, H. Feick, N. Tran, E. Weber, P. Yang, *Adv .Mater.* 13, 113 (2001).
18. K. Vanheusden, W.L. Warren, C.H. Ceager, D.R. Tallant, J.A.Voigt, *J. Appl. Phys.* 79, 7983 (1996).
19. M. Anpo, Y. Kubokawa, *J. Phys. Chem.* 88, 5556 (1984).